

Research Paper

# Stem Cell Labeling using Polyethylenimine Conjugated ( $\alpha$ -NaYbF<sub>4</sub>:Tm<sup>3+</sup>)/CaF<sub>2</sub> Upconversion Nanoparticles

Liang Zhao<sup>1,3,\*</sup>, Artem Kutikov<sup>2,\*</sup>, Jie Shen<sup>1</sup>, Chunying Duan<sup>3</sup>, Jie Song<sup>2</sup> and Gang Han<sup>1</sup>1. <sup>t</sup>Department of Biochemistry and Molecular Pharmacology, University of Massachusetts-Medical School, 364 Plantation Street, Worcester, Massachusetts 01605, United States.2. <sup>s</sup> Department of Orthopedics and Physical Rehabilitation, Department of Cell and Developmental Biology, University of Massachusetts Medical School, Worcester, Massachusetts 01605, United States.3. <sup>#</sup>State Key Laboratory of Fine Chemicals, Dalian University of Technology, Dalian, 116012, People's Republic of China.<sup>\*</sup> Equal contributions.

<sup>✉</sup> Corresponding author: Han G., Department of Biochemistry and Molecular Pharmacology, University of Massachusetts-Medical School, 364 Plantation Street, Worcester, Massachusetts 01605, United States. Phone: 508-856-3297 fax: 508-856-6231 e-mail: gang.han@umassmed.edu; Song J., Department of Orthopedics and Physical Rehabilitation, Department of Cell and Developmental Biology, University of Massachusetts Medical School, Worcester, Massachusetts 01605, United States. Phone: 508-334-7168 fax: 508-334-2770 e-mail: Jie.song@umassmed.edu.

© Ivyspring International Publisher. This is an open-access article distributed under the terms of the Creative Commons License (<http://creativecommons.org/licenses/by-nc-nd/3.0/>). Reproduction is permitted for personal, noncommercial use, provided that the article is in whole, unmodified, and properly cited.

Received: 2012.10.22; Accepted: 2012.12.23; Published: 2013.03.20

## Abstract

We report on a polyethylenimine (PEI) covalently conjugated ( $\alpha$ -NaYbF<sub>4</sub>:Tm<sup>3+</sup>)/CaF<sub>2</sub> upconversion nanoparticle (PEI-UCNP) and its use for labeling rat mesenchymal stem cells (rMSCs). The PEI-UCNPs absorb and emit near-infrared light, allowing for improved *in vivo* imaging depth over conventional probes. We found that such covalent surface conjugation by PEI results in a much more stable PEI-UCNP suspension in PBS compared to conventional electrostatic layer by layer (LbL) self-assembling coating approach. We systematically examined the effects of nanoparticle dose and exposure time on rat mesenchymal stem cell (rMSC) cytotoxicity. The exocytosis of PEI-UCNPs from labeled rMSCs and the impact of PEI-UCNP uptake on rMSC differentiation was also investigated. Our data show that incubation of 100- $\mu$ g/mL PEI-UCNPs with rMSCs for 4 h led to efficient labeling of the MSCs, and such a level of PEI-UCNP exposure imposed little cytotoxicity to rMSCs (95% viability). However, extended incubation of PEI-UCNPs at the 100  $\mu$ g/mL dose for 24 hour resulted in some cytotoxicity to rMSCs (60% viability). PEI-UCNP labeled rMSCs also exhibited normal early proliferation, and the internalized PEI-UCNPs did not leak out to cause unintended labeling of adjacent cells during a 14-day transwell culture experiment. Finally, PEI-UCNP labeled rMSCs were able to undergo osteogenic and adipogenic differentiation upon *in vitro* induction, although the osteogenesis of labeled rMSCs appeared to be less potent than that of the unlabeled rMSCs. Taken together, PEI-UCNPs are promising agents for stem cell labeling and tracking.

**Key words:** Near Infrared, Photoluminescence, Bioimaging, Upconversion Nanoparticles, Stem cell.

## Introduction

Mesenchymal stem cells (MSCs) are multipotent cells that can differentiate into a number cell types.

This technology holds great promise in a variety of life-threatening disease treatments such as diabetes

[1], cardiovascular disease [2], spinal-cord injuries [3] and cancers [4]. In order to facilitate their therapeutic use, the migration and differentiation of transplanted stem cells must be monitored over time with high spatial resolution. Optical imaging has emerged as a promising method for cell labeling due to its high sensitivity, cost-effectiveness, and rapid processing time. However, typical labeling agents such as organic dyes and fluorescent nanoparticles emit visible light with limited tissue penetration depth. To this end, many near infrared (NIR) emitting probes have been developed that take advantage of the elevated light penetration depth of NIR light. However, current NIR probes have drawbacks for *in vivo* tracking of stem cells. For example, synthetic NIR dyes are rapidly photobleached, making them ill-suited for longitudinal study of stem cell fate. Common NIR quantum dots (e.g., CdTe, InAs, PbS) are composed of highly toxic elements, limiting their clinical applications.

Lanthanide-doped upconversion nanoparticles (UCNPs) are promising materials for stem cell tracking due to their unique optical properties. Unlike traditional organic- [5-7] and protein-based materials [8], metal complexes [9-12] or semiconductor quantum dots [13, 14], these UCNPs generally have converse excitation and emission profiles: they are excited at NIR (980 nm), which is converted to a higher energy for emission at a visible or a shorter NIR wavelength [15, 16]. We have recently developed a novel biocompatible ( $\alpha$ -NaYbF<sub>4</sub>:Tm<sup>3+</sup>)/CaF<sub>2</sub> UCNP with enhanced NIR emission [17]. We demonstrated that such core/shell UCNPs are ideal for high contrast and deep tissue bioimaging. For example, they are completely free of autofluorescence for *in vitro* cell imaging and exhibit an exceptionally high signal-to-noise-ratio *in vivo* (i.e., 310 for Balb-c mice). The combination of NIR excitation and emission of this UCNP allows for outstanding tissue penetration depth (>3.2 cm), and it is 6-8 orders of magnitude brighter than conventional fluorescence based imaging probes in two-photon processes [18-22], with minimal light scattering and background from the surrounding tissue [23-25]. In addition, this nanoparticle is less toxic than quantum dots since they do not contain class I and class II toxic elements. The constituent ions of the shell of this UCNP, calcium and fluoride, are essentially endogenous elements in the living systems.

Proper surface modification of UCNPs is necessary to facilitate cellular uptake and subsequent applications for stem cell labeling. The intrinsic dynamic nature of cell surface antigen presentations on MSCs and the lack of unique cell surface markers or marker combinations for some animal MSCs (particularly

mouse MSCs) have made an antibody-based UCNPs surface modification and MSC targeting approach elusive. Surface modification of UCNPs with polycationic macromolecules enabling non-specific endocytosis are facile and practical, and have been the most commonly used strategy for shuttling nanoparticles across cell membranes for drug delivery or cell-labeling applications. Herein, we report on the development of a polyethylenimine (PEI)-conjugated ( $\alpha$ -NaYbF<sub>4</sub>:Tm<sup>3+</sup>)/CaF<sub>2</sub> UCNP. We evaluated its stability, cytotoxicity, cell uptake, exocytosis, and impact on cell proliferation and differentiation in regard to the labeling of rat mesenchymal stem cells (rMSCs).

## Materials and methods

### Materials

Yb<sub>2</sub>O<sub>3</sub> (99.9%), Tm<sub>2</sub>O<sub>3</sub> (99.9%), CF<sub>3</sub>COONa (99.9%), CF<sub>3</sub>COOH, CaCO<sub>3</sub>, 1-octadecene (90%), oleic acid (90%), diethylene glycol (99%), 1-Ethyl-3-(3-dimethylaminopropyl) carbodiimide hydrochloride (EDC-HCl), poly(acrylic acid) (PAA), N-hydroxysulfosuccinimide sodium salt (sulfo-NHS), NOBF<sub>4</sub> (97%) and branched polyethylenimine (PEI, Mw 25,000) were all purchased from Sigma-Aldrich and used without further purification. The trifluoroacetates of Yb and Tm were prepared as described [26].

### Instrumentation

The size and the morphology of the core and core/shell nanocrystals were characterized by transmission electron microscopy (TEM) using a JEM-2010 microscope at an acceleration voltage of 200 KV. The powder x-ray diffraction (XRD) patterns were recorded by a Siemens D500 diffractometer using Cu K $\alpha$  radiation ( $\lambda = 0.15418$  nm). The 2 $\theta$  angle of the XRD spectra was recorded at a scanning rate of 5°/minute. Upconversion photoluminescence (PL) spectra were recorded using a Fluorolog-3.11 Jobin Yvon spectrofluorimeter with a slit width defining a spectral resolution of 2 nm. The PL was excited at 975 nm using a fiber-coupled laser diode (Sheaumann, MA, USA) introduced to the sample chamber of the spectrofluorimeter. All upconversion PL spectra have been corrected for the spectral sensitivity of the system. Photographic images of upconverting nanocrystal colloids were taken with a digital camera (Canon Powershot SD800IS, Japan) without any filters.

### Synthesis of PEI-Coated Core/Shell $\alpha$ -(NaYbF<sub>4</sub>:0.5% Tm<sup>3+</sup>)/CaF<sub>2</sub> UCNPs

The hydrophobic oleic acid coated  $\alpha$ -(NaYbF<sub>4</sub>:0.5% Tm<sup>3+</sup>)/CaF<sub>2</sub> UCNPs were fabricated

based on our previously reported approach [17]. The PEI modification on the UCNPs was carried out in a 3-step reaction (Scheme 1/Figure S1). In the first step, oleic acid ligands on the UCNPs surface were removed using a nitrosonium tetrafluoroborate approach ( $\text{NOBF}_4$ ) [27]. During this reaction, 5 mL of oleic acid coated UCNPs dispersion in hexane (~5 mg/mL) was mixed with a 5 mL dichloromethane solution of  $\text{NOBF}_4$  (0.01 M) at room temperature. The resulting mixture was shaken gently, typically for 10 hours, until the precipitation of the UCNPs was observed. After centrifugation to remove the supernatant, the precipitated UCNPs were re-dispersed in dimethylformamide (DMF). In order to purify the UCNPs, toluene and hexane (1:1 v/v) were added to flocculate the UCNPs dispersion. After centrifugation, DMF was added to re-disperse the UCNPs, forming a stable colloidal dispersion. In the second step, 150 mg of PAA was added into a DMF dispersion of  $\text{NOBF}_4$ -treated UCNPs (5 mL, ~5 mg/mL) followed by vigorous stirring at 80 °C. After 30 minutes, the nanoparticles were precipitated by the addition of acetone and re-dispersed in water to form a stable dispersion. In the third step, the PAA-capped UCNPs were covalently grafted with branched PEI. 30 mg of PAA-capped UCNPs in 5 mL of DI water were activated by 1-Ethyl-3-(3-dimethylaminopropyl) carbodiimide hydrochloride (EDC-HCl, 50 mg) and sulfo-NHS (5 mg) in order to form the succinimidyl ester.

PEI (20 mg) in PBS buffer (2 mL) was then added to the reaction. After 2 hours of incubation at room temperature, the PEI-conjugated UCNPs (PEI-UCNPs) were purified by centrifugation and re-dispersion in DI water (5 mL). The electrostatic layer-by-layer (LbL) self-assembled PEI coated UCNPs were synthesized as follows. PAA-capped UCNPs (30 mg) in 5 mL of DI water were mixed with PEI (20 mg) in a PBS buffer (2 mL). After 2 hours of incubation at room temperature, the PEI LbL assembled UCNPs were purified by centrifugation and re-dispersion in DI water (5 mL).

### Isolation and culture of rat bone marrow stromal cells

All animal procedures were conducted in accordance with the principles and procedures approved by the University of Massachusetts Medical School Animal Care and Use Committee. Rat bone marrow cells were isolated from the long bones of a 4-week old male Charles River SASCO SD rat as previously described [28], and cultured in expansion media (ascorbic acid-free αMEM containing 20% FBS, 2% L-Glutamine, and 1% Penicillin-Streptomycin) at 37 °C and 5% CO<sub>2</sub>. After removing non-adherent cells on day 4 of the culture, adherent rat bone marrow stromal cells enriched for MSCs (rMSCs) were cultured to reach 80% confluence before being passaged.

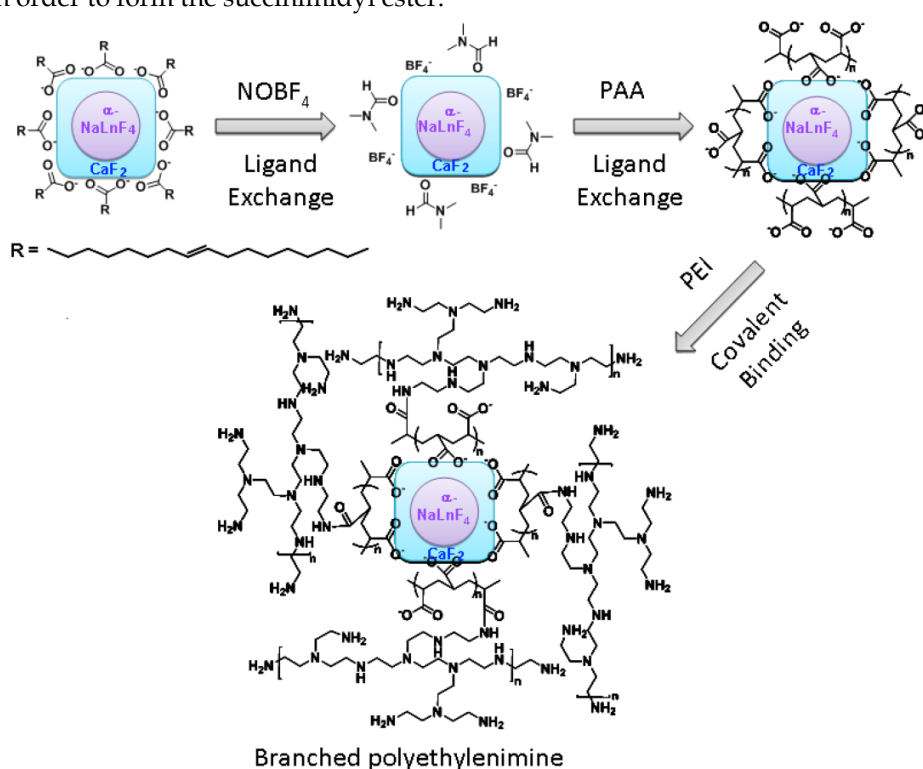


**Figure S1. (Scheme 1)** A surface modification scheme for PEI coated  $\alpha$ -(NaYbF<sub>4</sub>:0.5% Tm<sup>3+</sup>)@CaF<sub>2</sub> UCNPs.

## Cytotoxicity of PEI-UCNPs

Passage 1 rMSCs were seeded onto 96-well tissue culture plates ( $15,625/\text{cm}^2$  or  $5,000/\text{well}$ ) and cultured for 24-h prior to the addition of PEI-UCNPs (0, 20, 50 and  $100\ \mu\text{g}/\text{mL}$ ). Following 4 h or 24 h of incubation with PEI-UCNPs, the cells were washed 3 times with PBS to remove un-internalized PEI-UCNPs and fresh expansion media was added. Cytotoxicity of 4 h or 24 h treatment with PEI-UCNPs was quantified by MTT assay (Roche) 24 h after the initial UCNPs treatment. The effect of the 24 h UCNPs exposure on rMSC proliferation was further examined by MTT 48 h after the removal of un-internalized UCNPs. Three replicates were used for each experimental condition. Absorbance of the MTT product was read on a Multiskan FC microplate photometer (Thermo Scientific) at 570 nm with a 690nm background correction.

## Imaging of UCNPs-labeled rMSCs

Passage 1 rMSCS were seeded onto glass-bottom confocal dishes (MatTek Corp.,  $12,500/\text{cm}^2$ ) and cultured for 24 h prior to the addition of PEI-UCNPs (0, 50 or  $100\ \mu\text{g}/\text{mL}$  final concentration in media). The rMSCs were exposed to the particles for 4 or 24 h before the un-internalized PEI-UCNPs were removed by washing the cells 3 times with PBS. The cells were fixed by 3.7 v/v% methanol-free formaldehyde in PBS for 10 min and washed 3 times in PBS. Fixed cells were permeabilized with Triton X-100 (0.1% in PBS) for 5 min, washed with PBS, and then incubated in PBS containing 1% BSA for 30 min. Actin was stained with 2 units of Alexa Fluor 488-phalloidin (Invitrogen) in PBS containing 1% BSA for 20 min. Cell nuclei were stained with 300 nM of DAPI (Invitrogen) for 5 min. Cytoskeletal actin, UCNPs uptake, and cell nuclei were visualized under a 2-photon microscope (Zeiss LSM 7 MP with W Plan-Apochromatic 20X objective) with 870-nm excitation for Alexa Fluor 488 phalloidin, 980-nm excitation for the UCNPs, and 690-nm excitation for DAPI, respectively.

## PEI-UCNP exocytosis from rMSCs

A transwell system was used to study whether the internalized PEI-UCNPs were released from the rMSCs. The PEI-UCNP labeled rMSCs (4-h incubation with  $100\ \mu\text{g}/\text{mL}$  particles) were cultured on the transwell insert (the upper compartment;  $3.0\ \mu\text{m}$  pore size, polyester membrane). Unlabeled rMSCs were cultured in the underlying plate well (the lower compartment). The same cell seeding density of  $10,000\ \text{rMSCs}/\text{cm}^2$  were applied for both top and bottom compartments. The labeled and unlabeled cells were co-cultured for up to 14 days prior to fixation, DAPI staining, and imaging as described above. To confirm that PEI-UCNPs can pass through the

transwell membrane, PEI-UCNPs ( $100\ \mu\text{g}/\text{mL}$ ) were added to a cell-free control upper compartment and the rMSCs on the bottom compartment were imaged after 24 h.

## Induced differentiations of PEI-UCNP labeled rMSCs

Passage 1 rMSCs ( $10,500\ \text{cells}/\text{cm}^2$ ) were seeded onto a 12-well plate and cultured until they reached 70% confluence. rMSCs were labeled by 4-h incubation with PEI-UCNPs ( $100\ \mu\text{g}/\text{mL}$ ) followed by 3 washes with PBS. Osteogenic differentiation was induced by supplementing the expansion media with 10-nM dexamethasone, 20-mM  $\beta$ -glycerol phosphate, and  $50\text{-}\mu\text{M}$  L-ascorbic acid 2-phosphate. Adipogenic differentiation was induced by supplementing the expansion media with  $0.5\text{-}\mu\text{M}$  dexamethasone,  $0.5\text{-}\mu\text{M}$  isobutylmethylxanthine, and  $50\text{-}\mu\text{M}$  indomethacin. The rMSCs were differentiated for 14 days, with changes of differentiation media twice a week, and fixed. Osteogenic differentiation was visualized by Alizarin Red S staining for mineral deposition. Adipogenic differentiation was visualized by staining lipid deposits with Oil Red O. MSCs without UCNPs labels were cultured, induced to differentiate, and stained in the same manner. Staining specificity was validated by negative Alizarin Red S staining of cells following adipogenic induction and negative Oil Red O staining of cells following osteogenic induction.

## Results

### Synthesis and characterization of PEI-UCNPs

PEI was coupled to the surface of the UCNPs by covalent conjugation with the PAA. The nanoparticles formed a clear, aggregate free, solution in the PBS buffer. The PEI coating preserved the upconversion emissions in regard to both visible and near infrared regions (Figure 1A). When excited with a 980nm NIR laser diode, we observed strong upconversion luminescence emitted from the nanoparticles in the PBS buffer with the naked eye (Figure 1B). TEM imaging showed that the PEI-UCNPs are monodispersed in size (Figure 1C). In contrast to the electrostatic LbL self-assembly approach, we found that covalently bound PEI resulted in significantly enhanced stability of the PEI-UCNPs. Dynamic light scattering measurement showed that the hydrodynamic nanoparticle size of this covalently bonded PEI-UCNP was almost identical before and after 24-h incubation in PBS (~91nm), while the size of LbL self-assembled PEI-UCNPs increased from ~100nm to ~1um in 5 hours (Figure 2A). The FT-IR measurements suggested the successful PEI conjugation due to the appearance of N-H bending peaks. (Figure 2B) Zeta po-

tential measurement of the PEI-UCNPs further confirmed the presence of a PEI surface coating with a positive potential of approximately +17.8 mV(i.e., in

comparison with -31 mV of PAA-UCNPs), which would be suitable for binding with negatively charged cell surfaces.

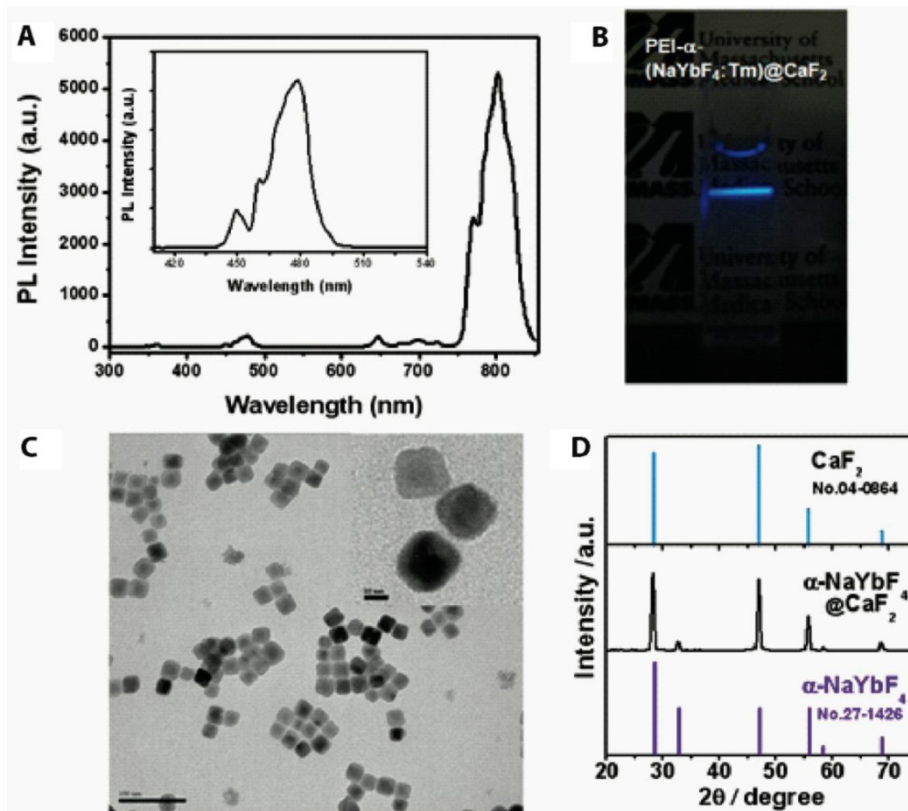
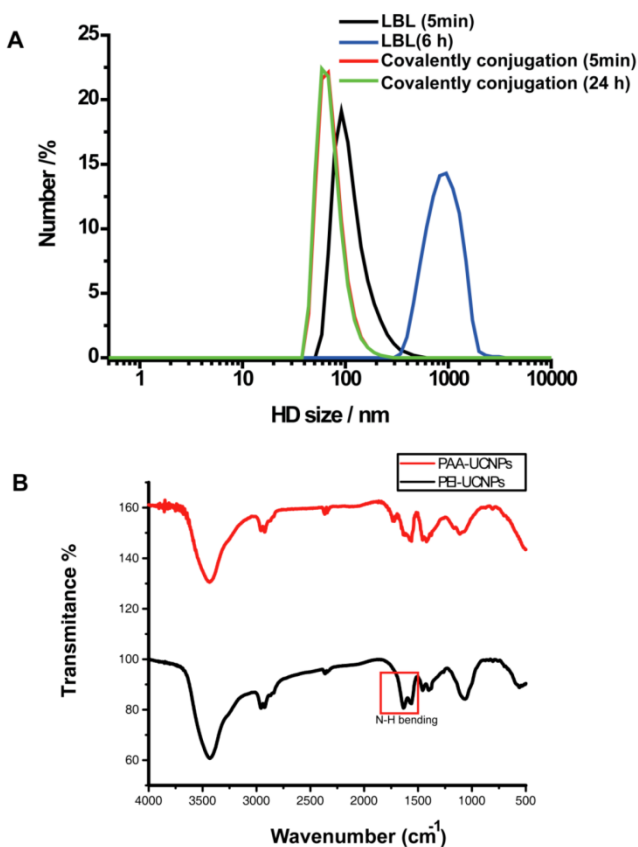


**Figure 2.** (A) The hydrodynamic (HD) size distributions of covalently conjugated and LbL self assembled PEI-UCNPs. (B) Plot of FT-IR of PAA-UCNPs and PEI-UCNPs.



### PEI-UCNP cellular uptake and cytotoxicity

In order to determine the optimal time and nanoparticle concentration for stem cell labeling, rMSCs were treated with different concentrations of PEI-UCNPs (0, 20, 50, or 100  $\mu\text{g}/\text{mL}$ ) for 4 h and 24 h. After incubation, the cells were washed and imaged using a 2-photon microscope. The upconversion luminescence was observed in nearly all of the rMSCs, demonstrating that the stem cells were successfully labeled with the PEI-UCNPs. The level of PEI-UCNP uptake in individual cells was proportional to the nanoparticle treatment concentration and exposure time (Figure 3A). Co-staining for cytoskeletal actin and nuclei further validated the localization of PEI-UCNP signal within the cytoplasm of rMSCs (Figure 3B).

We next examined the cytotoxicity of the nanoparticle at the aforementioned concentrations and time points. The MTT assay showed that nearly 95% of rMSCs were viable following a 4 h nanoparticle exposure at concentrations up to 100  $\mu\text{g}/\text{mL}$ . There

was no significant difference in cell viability between the PEI-UCNP labeled groups and unlabeled control ( $p > 0.05$ ). When the exposure time was increased to 24 h, the cell viability significantly decreased compared to the unlabeled control at each concentration examined, with a 63% reduction at the treatment concentration of 100  $\mu\text{g}/\text{mL}$  (Figure 3C). There was no significant difference in toxicity between 50  $\mu\text{g}/\text{mL}$  and 100  $\mu\text{g}/\text{mL}$  doses at this exposure time. To investigate the impact of PEI-UCNP labeling on the proliferation capability of rMSCs, rMSCs were incubated with PEI-UCNPs at various concentrations for 24 h. After removal of un-internalized UCNPs, the cells were cultured for another 48 h before being subjected to MTT assay. The short-term proliferation of rMSCs was minimally impacted by the PEI-UCNP labeling. All groups exhibited significant increases in the number of viable cells, with 1.84-fold increase in viable cells for rMSCs treated with 100  $\mu\text{g}/\text{mL}$  of PEI-UCNPs after 48 h culture as compared to 1.79-fold increase for unlabeled rMSCs (Figure 3D).

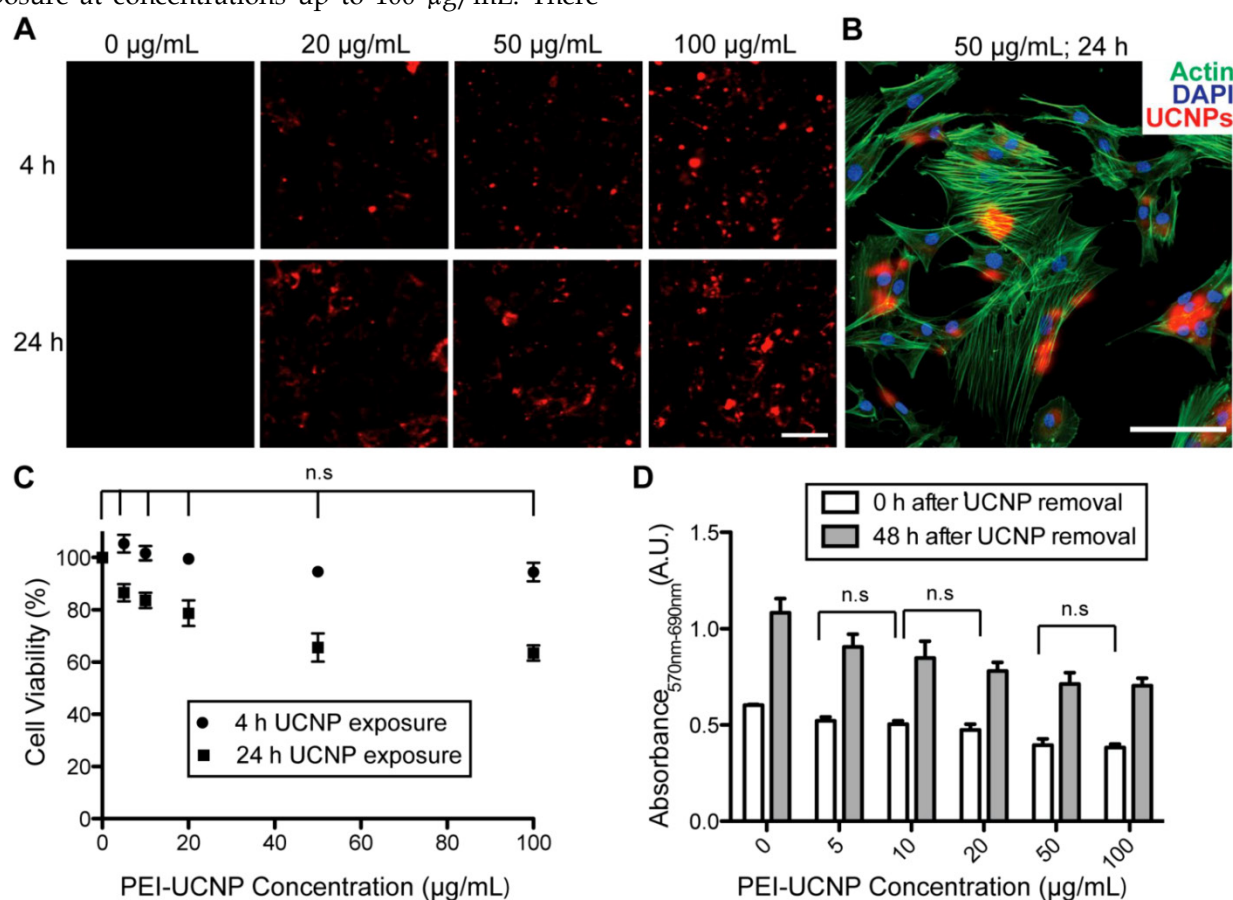


**Figure 3.** The uptake efficiency of PEI-UCNPs by rMSCs and the viability and proliferation of labeled rMSCs. (A) Two-photon microscopy images of rMSCs following 4-h and 24-h incubation with various concentrations of PEI-UCNPs. Scale bar = 50  $\mu\text{m}$  (B) Co-localization of UCNP signal with rMSC actin and nuclei following incubation with 50  $\mu\text{g}/\text{mL}$  UCNPs for 24 h. Scale bar = 50  $\mu\text{m}$  (C) rMSC viability following 4 h and 24 h incubation with various concentrations of PEI-UCNPs. Percent viability is calculated relative to the MTT absorbance of unlabeled rMSCs. (D) The impact of PEI-UCNP labeling on rMSC proliferation as determined by MTT assay. Significance of statistical comparisons were determined by one-way ANOVA with Tukey post-hoc. All pairwise comparisons are significant ( $p < 0.05$ ) unless denoted as n.s. ( $p > 0.05$ , not significant).

## Exocytosis of PEI-UCNPs from labeled rMSCs

One potential challenge for *in vivo* tracking of UCNPs-labeled stem cells is the possibility that the taken nanoparticles could be exocytosed overtime, leading to the unintended labeling of other surrounding cells. We investigated this issue using a transwell culture system[29] where rMSCs labeled with PEI-UCNPs (100 µg/mL, 4h) were cultured on the porous membrane in the upper compartment while the unlabeled rMSCs were cultured in the lower compartment (Figure 4A). PEI-UCNPs added to a cell-free upper compartment were able to quickly pass through the membrane and cause the labeling of rMSCs seeded in the lower compartment in 1 day (Figure 4B, control). The labeled and unlabeled cells were co-cultured for 14 days and the cells in the bottom compartment remained free of any PEI-UCNP signal throughout this culture period, supporting that there was no particles excreted from the labeled cells in the upper compartment (Figure 4D).

## Differentiation of PEI-UCNP labeled rMSCs

The effect of PEI-UCNP labeling on the osteogenic and adipogenic differentiations of rMSCs were assessed. Passage 1 rMSCs labeled with PEI-UCNPs (100 µg/mL, 4 h) were cultured in osteogenic or adipogenic media for 14 days and their differentiation potency was compared with that of unlabeled MSCs. Light microscopy shows that the PEI-UCNP labeled rMSCs were able to undergo osteogenic and adipogenic differentiation as supported by the positive Alizarin Red S (Figure 5A) and Oil Red O (Figure 5B) staining, respectively. The intensity of Alizarin red S

staining, however, was reduced for the PEI-UCNP labeled rMSCs compared to the unlabeled control (Figure 5A).

## Discussion

The ability to label and track stem cells has far reaching applications in tissue engineering and regenerative medicine, where the fate of implanted stem cells remains unclear. Stem cell labeling with NIR probes has the potential to allow for the *in vivo* study of stem cell fate with greater tissue penetration depth and spatial resolution than conventional cell labeling methods. Herein, we report the application of a recently developed UCNPs with NIR-excitation and NIR-emission to the labeling of rMSCs.

We compared two approaches of modifying the surface of the UCNPs with PEI, facilitating non-specific cellular uptake. In one approach, we used an LbL method that deposits PEI by electrostatic interactions around the nanoparticle surface. In a second approach, we covalently coupled the PEI to the UCNPs surface through a PAA intermediate. The presence of a PEI coating was confirmed by zeta potential measurements that indicated a positive charge on the particle surface. We found that the covalently linked PEI resulted in increased particle stability, with no increase in hydrodynamic size over the course of a 24 h incubation in PBS. In contrast, the LbL assembled PEI resulted in rapid particle aggregation in PBS. Due to their increased stability, we chose the UCNPs with the covalently coupled PEI coating (PEI-UCNPs) for further cell-based analysis.

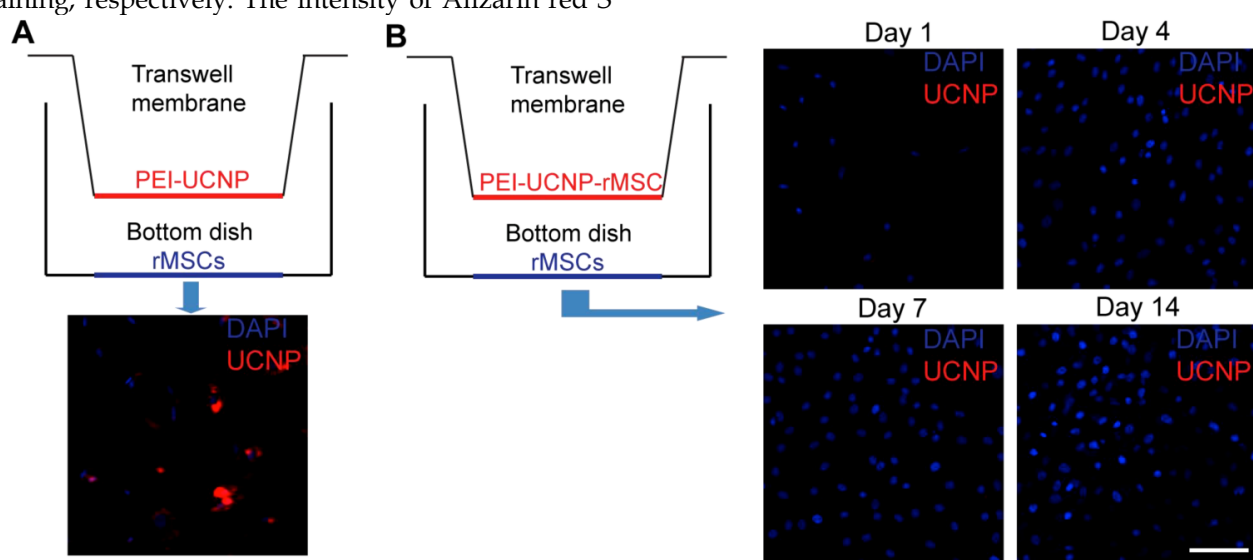


**Figure 4.** Exocytosis of PEI-UCNPs by labeled rMSCs. (A) Schematic of a control transwell setup containing PEI-UCNPs on the top well membrane and rMSCs on the bottom well, and the two-photon imaging of the bottom dish rMSCs. (B) Schematic of a transwell co-culture setup containing PEI-UCNP labeled rMSCs on top well membrane and unlabeled rMSCs on the bottom dish, and the two-photon imaging of the bottom dish rMSCs over a 14 day period. Cell nuclei were stained with DAPI. Scale bar = 50 µm.

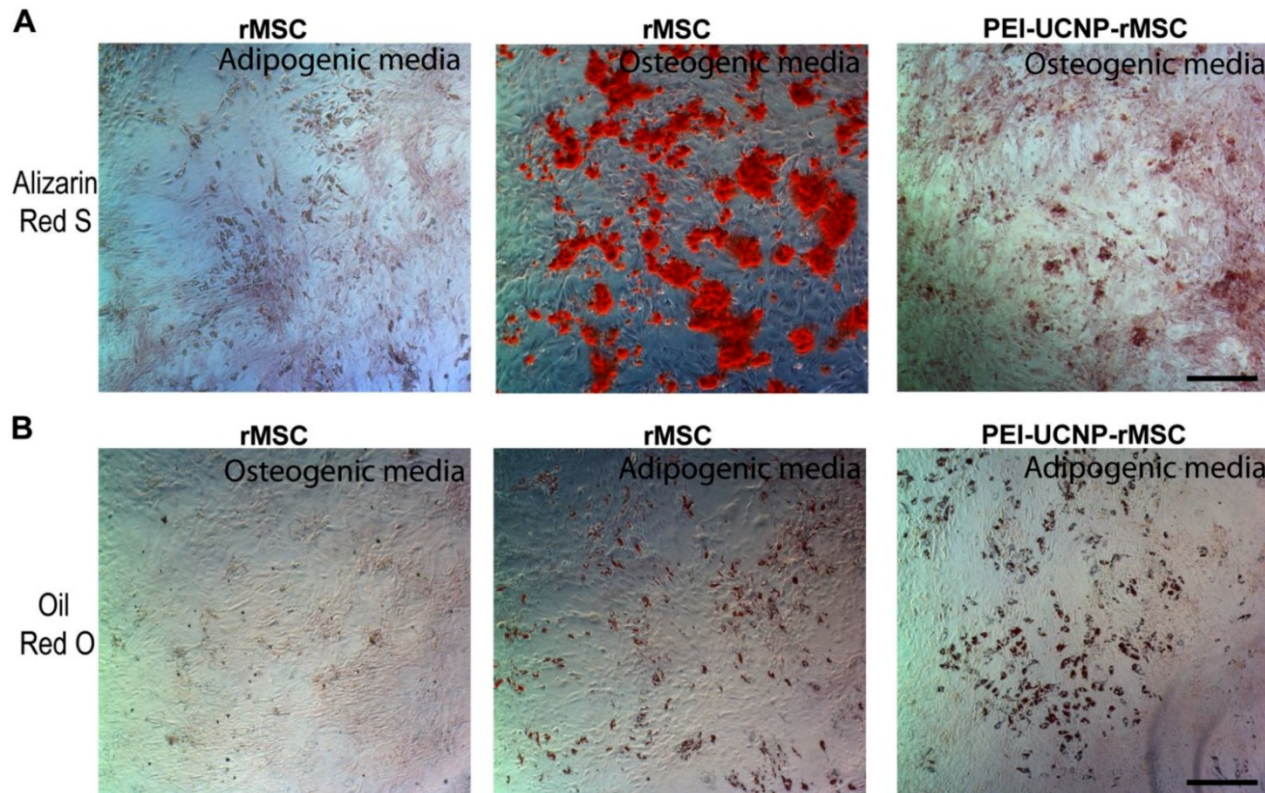


**Figure 5.** Osteogenic and adipogenic differentiation of PEI-UCNP labeled rMSCs. (A) Alizarin red S staining of unlabeled rMSCs after 14-day culture in adipogenic (negative staining control) and osteogenic media (positive control), and labeled rMSCs after 14-day culture in osteogenic media. Scale bar = 100  $\mu$ m. (B) Oil red O staining of unlabeled rMSCs after 14-day culture in osteogenic (negative staining control) and adipogenic media (positive control), and labeled rMSCs after 14-day culture in adipogenic media. Scale bar = 100  $\mu$ m.

We used rMSCs as a model to determine the efficacy of PEI-UCNPs for stem cell labeling. MSCs are a multipotent cell that can differentiate into osteoblasts, chondrocytes, myocytes and adipocytes. They have been studied widely for musculoskeletal tissue engineering and have been used clinically.[30-32] Tracking labeled MSCs *in vivo* is important for the validation and development of MSC-based therapeutic strategies. We show that the PEI-UCNP concentration and incubation-time can be optimized to achieve efficient rMSCs labeling with negligible cytotoxicity. Specifically, we showed that a 4 h incubation with 100  $\mu$ g/mL PEI-UCNPs effectively labeled rMSCs while maintaining ~95% cell viability. Although a longer exposure of 24 h did lead to increased cytotoxicity in a dose dependent manner, the cytotoxicity did appear to level off beyond a particle concentration of 50  $\mu$ g/mL. Further, UCNPs signals were localized to the rMSC cytoplasm and did not negatively impact the short-term (48 h) proliferation of MSCs.

Transwell coculture experiments showed that PEI-UCNP internalized in the rMSCs did not leak out via exocytosis during a 14-day period to cause unintended labeling of surrounding cells. This supports

the feasibility of *in vivo* cell tracking over a couple of weeks without causing non-specific secondary labeling of other cells. Finally, we showed that PEI-UCNP labeled rMSCs were able to differentiate along the osteogenic and adipogenic lineages upon *in vitro* induction, suggesting that the PEI-UCNP labeling did not abolish these key functions of MSCs. Although the PEI-UCNP labeled rMSCs exhibited less potent osteogenic differentiation than the unlabeled control, the potency of adipogenic differentiation was largely unaffected by PEI-UCNP labeling. It remains to be seen whether other lineage commitments and *in vivo* differentiation of MSCs is affected by the PEI-UCNP labeling. Finally, the observed impact on the osteogenic differentiation potency of PEI-UCNP labeled rMSCs may be further minimized by exploring even more cytocompatible surface coating strategies.

## Conclusions

The NIR-excitation and NIR-emission of  $\alpha$ -NaYF<sub>4</sub>:Yb<sup>3+</sup>,Tm<sup>3+</sup>/CaF<sub>2</sub> UCNPs allows for increased tissue penetration depth, facilitating *in vivo* imaging. We report the development of core/shell  $\alpha$ -NaYF<sub>4</sub>:Yb<sup>3+</sup>,Tm<sup>3+</sup>/CaF<sub>2</sub> UCNPs with a covalently

coupled PEI coating (PEI-UCNPs) and their validation for stem cell labeling applications. We show that the covalently coupled PEI coating results in greater particle stability in PBS than UCNPs coated with PEI using a layer-by-layer approach. The PEI-UCNPs show reasonable cytocompatibility at a concentration and exposure time adequate for efficient labeling of rMSCs. The cell viability remained above 95% after a 4 h PEI-UCNP exposure at 100 µg/mL. Further, the PEI-UCNP labeling did not impair short-term cell proliferation. Exocytosis of internalized PEI-UCNP from labeled cells was not observed during a 14-day culture period. Finally, PEI-UCNPs labeled rMSCs were able to undergo osteogenic and adipogenic differentiations upon in vitro induction, although the potency of the former was reduced compared to unlabeled control. Taken together, PEI-UCNPs have promising applications in cell labeling and *in vivo* tracking.

## Acknowledgements

G.H. thanks for the start up fund of University of Massachusetts Medical School and the Worcester Foundation Mel Cutler Award, and UMASS Commercial Ventures & Intellectual Property (CVIP) award. L. Z. gratefully acknowledges support from the China Scholarship Council for the State Scholarship Fund.

## Abbreviations

PEI: polyethylenimine; UCNPs: upconversion nanoparticle; rMSCs : rat mesenchymal stem cells; LbL: layer by layer; NIR: near infrared ; EDC-HCl :1-Ethyl-3-(3-dimethylaminopropyl) carbodiimide hydrochloride; PAA: poly(acrylic acid) ; Sulfo-NHS: N-hydroxysulfosuccinimide sodium salt; NOBF<sub>4</sub>: nitrosonium tetrafluoroborate; PL: photoluminescence; DMF: dimethylformamide.

## Competing Interests

The authors have declared that no competing interest exists.

## References

- Assady S, Maor G, Amit M, Itskovitz-Eldor J, Skorecki KL, Tzukerman M. Insulin production by human embryonic stem cells. *Diabetes*. 2001; 50: 1691-7.
- Cao F, Lin S, Xie XY, Ray P, Patel M, Zhang XZ, et al. In vivo visualization of embryonic stem cell survival, proliferation, and migration after cardiac delivery. *Circulation*. 2006; 113: 1005-14.
- McDonald JW, Liu XZ, Qu Y, Liu S, Mickey SK, Turetsky D, et al. Transplanted embryonic stem cells survive, differentiate and promote recovery in injured rat spinal cord. *Nat Med*. 1999; 5: 1410-2.
- Singh SK, Hawkins C, Clarke ID, Squire JA, Bayani J, Hide T, et al. Identification of human brain tumour initiating cells. *Nature*. 2004; 432: 396-401.
- Terai T, Nagano T. Fluorescent probes for bioimaging applications. *Curr Opin Chem Biol*. 2008; 12: 515-21.
- Beija M, Afonso CAM, Martinho JMG. Synthesis and applications of Rhodamine derivatives as fluorescent probes. *Chem Soc Rev*. 2009; 38: 2410-33.
- Zhang M, Yu MX, Li FY, Zhu MW, Li MY, Gao YH, et al. A highly selective fluorescence turn-on sensor for Cysteine/Homocysteine and its application in bioimaging. *J Am Chem Soc*. 2007; 129: 10322-3.
- Giepmans BNG, Adams SR, Ellisman MH, Tsien RY. Review - The fluorescent toolbox for assessing protein location and function. *Science*. 2006; 312: 217-24.
- Zhao L, Qu SY, He C, Zhang R, Duan CY. Face-driven octanuclear cerium(IV) luminescence polyhedra: synthesis and luminescent sensing natural saccharides. *Chem Commun*. 2011; 47: 9387-9.
- Zhao Q, Huang CH, Li FY. Phosphorescent heavy-metal complexes for bioimaging. *Chem Soc Rev*. 2011; 40: 2508-24.
- Lo KK, Li SPY, Zhang KY. Development of luminescent iridium(III) polypyridine complexes as chemical and biological probes. *New J Chem*. 2011; 35: 265-87.
- Eliseeva SV, Bunzli JCG. Lanthanide luminescence for functional materials and bio-sciences. *Chem Soc Rev*. 2010; 39: 189-227.
- Michalet X, Pinaud FF, Bentolila LA, Tsay JM, Doose S, Li JJ, et al. Quantum dots for live cells, *in vivo* imaging, and diagnostics. *Science*. 2005; 307: 538-44.
- Wang QB, Liu Y, Ke YG, Yan H. Quantum dot bioconjugation during core-shell synthesis. *Angew Chem Int Edit*. 2008; 47: 316-9.
- Chen F, Bu WB, Zhang SJ, Liu XH, Liu JN, Xing HY, et al. Positive and Negative Lattice Shielding Effects Co-existing in Gd (III) Ion Doped Bifunctional Upconversion Nanoprobes. *Adv Funct Mater*. 2011; 21: 4285-94.
- Xing HY, Bu WB, Ren QG, Zheng XP, Li M, Zhang SJ, et al. A NaYbF<sub>4</sub>: Tm<sup>3+</sup> nanoprobe for CT and NIR-to-NIR fluorescent bimodal imaging. *Biomaterials*. 2012; 33: 5384-93.
- Chen G, Shen J, Ohulchansky YY, Patel NJ, Kutikov A, Li Z, et al. (alpha-NaYbF<sub>4</sub>):Tm<sup>3+))/CaF<sub>2</sub>) Core/Shell Nanoparticles with Efficient Near-Infrared to Near-Infrared Upconversion for High-Contrast Deep Tissue Bioimaging. *Acs Nano*. 2012; 6: 8280-7.</sup>
- Wang F, Banerjee D, Liu YS, Chen XY, Liu XG. Upconversion nanoparticles in biological labeling, imaging, and therapy. *Analyst*. 2010; 135: 1839-54.
- Mader HS, Kele P, Saleh SM, Wolfbeis OS. Upconverting luminescent nanoparticles for use in bioconjugation and bioimaging. *Curr Opin Chem Biol*. 2010; 14: 582-96.
- Chatterjee DK, Gnanasamandhan MK, Zhang Y. Small Upconverting Fluorescent Nanoparticles for Biomedical Applications. *Small*. 2010; 6: 2781-95.
- Zhou J, Liu Z, Li FY. Upconversion nanophosphors for small-animal imaging. *Chem Soc Rev*. 2012; 41: 1323-49.
- Shen J, Zhao L, Han G. Lanthanide-doped upconverting luminescent nanoparticle platforms for optical imaging-guided drug delivery and therapy. *Adv Drug Deliv Rev*. 2012; [Epub ahead of print].
- Frangioni JV. *In vivo* near-infrared fluorescence imaging. *Curr Opin Chem Biol*. 2003; 7: 626-34.
- Hilderbrand SA, Weissleder R. Near-infrared fluorescence: application to *in vivo* molecular imaging. *Curr Opin Chem Biol*. 2010; 14: 71-9.
- Gao JH, Chen XY, Cheng Z. Near-Infrared Quantum Dots as Optical Probes for Tumor Imaging. *Curr Top Med Chem*. 2010; 10: 1147-57.
- Roberts JE. Lanthanum and Neodymium Salts of Trifluoroacetic Acid. *J Am Chem Soc*. 1961; 83:1087-8.
- Dong AG, Ye XC, Chen J, Kang YJ, Gordon T, Kikkawa JM, et al. A Generalized Ligand-Exchange Strategy Enabling Sequential Surface Functionalization of Colloidal Nanocrystals. *J Am Chem Soc*. 2011; 133: 998-1006.
- Song J, Xu JW, Filion T, Saiz E, Tomsia AP, Lian JB, et al. Elastomeric high-mineral content hydrogel-hydroxyapatite composites for orthopedic applications. *J Biomed Mater Res A*. 2009; 89A: 1098-107.
- Wang C, Cheng L, Xu H, Liu Z. Towards whole-body imaging at the single cell level using ultra-sensitive stem cell labeling with oligo-arginine modified upconversion nanoparticles. *Biomaterials*. 2012; 33: 4872-81.
- Satija NK, Singh VK, Verma YK, Gupta P, Sharma S, Afrin F, et al. Mesenchymal stem cell-based therapy: a new paradigm in regenerative medicine. *J Cell Mol Med*. 2009; 13: 4385-402.
- Abdallah BM, Kassem M. Human mesenchymal stem cells: from basic biology to clinical applications. *Gene Ther*. 2008; 15: 109-16.
- Giordano A, Galderisi U, Marino IR. From the laboratory bench to the patients bedside: An update on clinical trials with mesenchymal stem cells. *J Cell Physiol*. 2007; 211: 27-35.